



UNIVERSITÀ DI PARMA

ARCHIVIO DELLA RICERCA

University of Parma Research Repository

Vortex dynamics and irreversibility line in optimally doped SmFeAsO_{0.8}F_{0.2} from ac susceptibility and magnetization measurements

This is the peer reviewed version of the following article:

Original

Vortex dynamics and irreversibility line in optimally doped SmFeAsO_{0.8}F_{0.2} from ac susceptibility and magnetization measurements / G., Prando; P., Carretta; DE RENZI, Roberto; S., Sanna; A., Palenzona; M., Putti; M., Tropeano. - In: PHYSICAL REVIEW. B, CONDENSED MATTER AND MATERIALS PHYSICS. - ISSN 1098-0121. - 83:(2011), pp. 174514-1-174514-6. [10.1103/PhysRevB.83.174514]

Availability:

This version is available at: 11381/2346550 since:

Publisher:

Published

DOI:10.1103/PhysRevB.83.174514

Terms of use:

Anyone can freely access the full text of works made available as "Open Access". Works made available

Publisher copyright

note finali coverpage

(Article begins on next page)

Vortex dynamics and irreversibility line in optimally doped $\text{SmFeAsO}_{0.8}\text{F}_{0.2}$ from ac susceptibility and magnetization measurements

G. Prando,^{1,2} P. Carretta,¹ R. De Renzi,³ S. Sanna,¹ A. Palenzona,⁴ M. Putti,⁴ and M. Tropeano⁴

¹*Department of Physics "A. Volta," University of Pavia-CNISM, I-27100 Pavia, Italy*

²*Department of Physics "E. Amaldi," University of Rome Tre-CNISM, I-00146 Roma, Italy*

³*Department of Physics, University of Parma-CNISM, I-43124 Parma, Italy*

⁴*CNR-INFN-LAMIA and University of Genova, I-16146 Genova, Italy*

(Received 1 February 2011; revised manuscript received 24 March 2011; published 17 May 2011)

Ac susceptibility and static magnetization measurements were performed in the optimally doped $\text{SmFeAsO}_{0.8}\text{F}_{0.2}$ superconductor. The field-temperature phase diagram of the superconducting state was drawn, and, in particular, the features of the flux lines were derived. The dependence of the intragrain depinning energy on the magnetic field intensity was derived in the thermally activated flux-creep framework, enlightening a typical $1/H$ dependence in the high-field regime. The intragrain critical current density was extrapolated in the zero-temperature and zero-magnetic-field limit, showing a remarkably high value $J_{c0}(0) \sim 2 \times 10^7$ A/cm², which demonstrates that this material is rather interesting for potential future technological applications.

DOI: [10.1103/PhysRevB.83.174514](https://doi.org/10.1103/PhysRevB.83.174514)

PACS number(s): 74.25.Uv, 74.25.Wx, 74.70.Xa

I. INTRODUCTION

Several properties of iron-based 1111 oxypnictide superconductors like, for instance, the high crystallographic and superconducting anisotropy and large penetration depths make them similar to cuprate high- T_c materials. Since their discovery,^{1,2} several studies have been performed in order to clarify their intrinsic microscopic properties.^{3,4} The attention has been mainly focused on the bosonic coupling mechanism of the superconducting electrons, on the features of the spin density wave magnetic phase characterizing the parental and lightly doped compounds and its possible coexistence with superconductivity,⁵⁻⁷ and on the interaction between localized magnetism from rare-earth (RE) ions and itinerant electrons onto FeAs bands.⁸⁻¹⁰ A common hope is that a full comprehension of these topics in oxypnictide superconductors could also allow one to answer several open questions on the cuprates.

At the same time, other analogies with cuprates possibly characterize 1111 oxypnictides as interesting materials for technological applications, like small coherence lengths (and, correspondingly, high values of upper critical fields) besides the high values of the superconducting critical temperature T_c . In this respect, studies of macroscopic properties like critical fields and critical depinning currents are of the utmost importance. Namely, the investigation of the dynamical features of the flux lines (FLs) and of the so-called irreversibility line, typically investigated by means of both resistance and ac susceptibility measurements, is in order. Those measurements allow one to further check the validity of the theories used to model the mixed state of cuprate materials and, in particular, the vortices motion and its relationship with the possible pinning mechanisms.¹¹ Several works reporting magnetoresistance,¹²⁻¹⁴ modulated microwave absorption¹⁵ and dc magnetization¹⁶⁻¹⁹ examining the FLs dynamics in 1111 oxypnictides have already been published in the last two years. To our knowledge, no study of the FLs by means of ac susceptibility measurements has been published yet.

This paper deals with the field, temperature, and frequency dependences of ac susceptibility in optimally doped

$\text{SmFeAsO}_{0.8}\text{F}_{0.2}$, which is one of the compounds showing the highest T_c among all the iron-based superconductors. Although no large-enough single crystals are available and our data refer to unoriented powder samples, the power of the ac susceptibility technique allowed us to deduce several intrinsic features of the mixed state of the superconductor. The magnetic field (H) behavior of the irreversibility line was obtained, allowing to draw (together with dc magnetization data) a detailed phase diagram of the FLs. The H dependence of the intragrain effective depinning energy (U_0) was investigated, evidencing the characteristic crossover from a single-vortex dynamics to a collective dynamics ($U_0 \propto 1/H$) at a field $H \sim 0.5$ T. An estimate of the intragrain critical depinning current density in the limit of vanishing temperature and magnetic field was also deduced, giving the remarkably high value of $J_{c0}(0) \sim 2 \times 10^7$ A/cm². This result is of great importance in characterizing $\text{SmFeAsO}_{0.8}\text{F}_{0.2}$ as a superconductor suitable for technological applications.

II. EXPERIMENTALS AND MAIN RESULTS

$\text{SmFeAsO}_{0.8}\text{F}_{0.2}$ was prepared by solid state reaction at ambient pressure from Sm, As, Fe, Fe_2O_3 , and FeF_2 . SmAs was first synthesized from pure elements in an evacuated, sealed glass tube at a maximum temperature of 550 °C. The final sample was synthesized by mixing SmAs, Fe, Fe_2O_3 , and FeF_2 powders in stoichiometric proportions, using uniaxial pressing to make powders into a pellet and then heat treating the pellet in an evacuated, sealed quartz tube at 1000 °C for 24 h, followed by furnace cooling. The sample was analyzed by powder x-ray diffraction in a Guinier camera, with Si as the internal standard. The powder pattern showed the sample to be single phase with two weak extra lines at low angle of the SmOF extra phase. The lattice parameters were $a = 3.930(1)$ Å and $c = 8.468(2)$ Å.

Static magnetization M_{dc} measurements were performed by means of a Quantum Design MPMS-XL7 Superconducting Quantum Interference Device (SQUID) magnetometer. The temperature T dependence of M_{dc} upon field cooling (FC) the sample was monitored at different applied magnetic

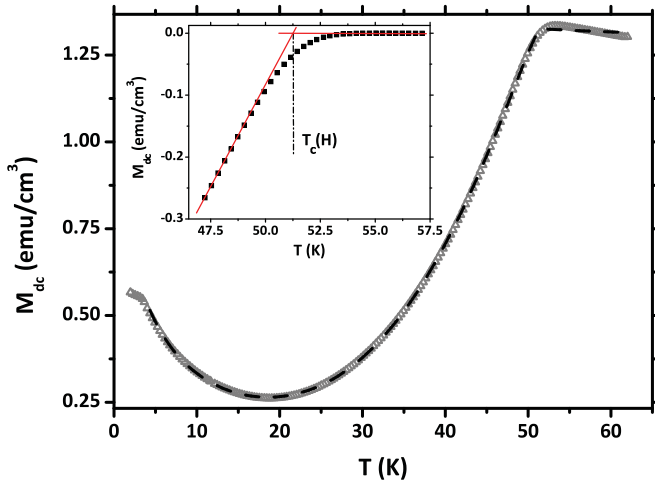


FIG. 1. (Color online) Temperature dependence of static magnetization M_{dc} on FC the sample at $H = 1.5$ T. Dashed lines are the best-fitting functions according to Eq. (2) (see later on in the text). Inset: estimate of $T_c(H = 1.5$ T) after the subtraction of the paramagnetic contribution.

fields up to 7 T. Representative raw M_{dc} vs. T curves are shown in Fig. 1. The superconducting (SC) response, with onset around $T_c \simeq 52$ K, is found to be superimposed to a paramagnetic contribution associated with Sm^{3+} ions. Clear kinks in the magnetization curves can be observed at $T_N \simeq 4$ K, evidencing the antiferromagnetic transition of the Sm^{3+} magnetic moments.²⁰ The field dependence of the SC transition temperature $T_c(H)$ was deduced by first subtracting the linear extrapolation of the Sm^{3+} paramagnetic contribution in a few-K region around the SC onset from the raw data. The transition temperatures were then estimated from the intersection of two linear fits of the resulting curves above and below the onset (see Fig. 1, inset). $T_c(H)$ behavior was also deduced by means of magnetoresistance measurements on the application of magnetic fields up to 9 T, showing a behavior analogous to what was observed in $\text{SmFeAsO}_{1-x}\text{F}_x$ compounds from the same batch but with lower x concentrations of F^- .²¹

The onset of the diamagnetic contribution and its dependence on the applied external magnetic field was also investigated by means of a Quantum Design MPMS-XL5 SQUID ac susceptometer. Measurements were performed with an alternating field in the range $H_{ac} = (0.0675 - 1.5) \times 10^{-4}$ T parallel to the static field H , which varied up to 5 T. The ac field frequency ranged from 37 to 1488 Hz. The diamagnetic onset temperature was estimated from χ' vs. T curves by means of the same procedure shown in the inset of Fig. 1.

An accurate examination of ac susceptibility data as a function of the ac working frequency ν_m allowed us to obtain further information on the dynamical properties of the FLs. It is well known, in fact, that a peak in χ'' vs. T curves associated with a maximum in the energy dissipation inside the sample appears at a temperature T_p slightly lower than the diamagnetic onset temperature in χ' . Correspondingly, at the same temperature T_p the χ' vs. T curve displays a maximum in its first derivative²² (see exemplifying raw data in Fig. 2, lower panel). Several works in the past decades have tried to clarify

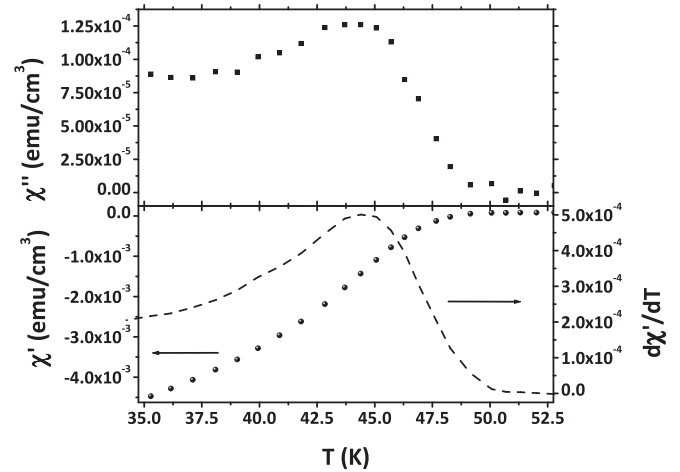


FIG. 2. Temperature dependence of the real and imaginary components of ac susceptibility χ' and χ'' (bottom and top panels, respectively). The alternating field amplitude $H_{ac} = 1.5 \times 10^{-4}$ T at the frequency $\nu_m = 37$ Hz is superimposed to a larger static field $H = 1.5$ T. The dashed line in the bottom panel represents the first derivative of χ' with respect to temperature.

the origin of the χ'' peak. One of the possible interpretations relies on the Bean's critical state model^{23,24} and associates the peak in χ'' with the flux front reaching the center of the sample. In this case, the peak temperature T_p should not depend on the measurement frequency ν_m , and a strong dependence on sample dimensions and ac field amplitude H_{ac} are predicted.²⁵ Another interpretation relies on the modification of the skin depth, due to the superconductor resistivity in the thermally assisted flux-flow (TAFF) regime with respect to the London penetration depth. In this case T_p should strongly depend on the measurement frequency ν_m while no dependence on the ac field amplitude H_{ac} is predicted.^{22,25-29} Considering the frequency dependence of the χ'' peak, another interesting interpretation has been associated with a resonant absorption of energy obtained when the inverse of ν_m matches the characteristic relaxation time τ_c of the FL at T_p ,^{30,31} namely

$$2\pi \nu_m \tau_c|_{T=T_p} = 1. \quad (1)$$

In this case, the underlying theory is the more general framework of the thermally activated creep of FLs between different metastable minima of pinning potentials.^{32,33}

At temperatures lower than T_p , other broader contributions to both χ' and χ'' were found and interpreted as arising from granularity of the powder sample and, in particular, to intergranular Josephson weak links between different grains.^{29,34,35} In cuprate materials, from the analysis of the low-temperature peak in χ'' and, in particular, of its frequency dependence, the depinning energy barrier associated with grain boundaries was extracted.^{34,36,37} Strong granularity has been observed also in iron-based pnictide materials. On samples prepared with the same procedure a small (though not negligible) intergranular critical density current has been evaluated by a remanent magnetization analysis.³⁸ However, it has been determined that the main contribution to the magnetization curve comes from intragranular currents. By considering our data just in the T region close enough to the diamagnetic onset, then, we

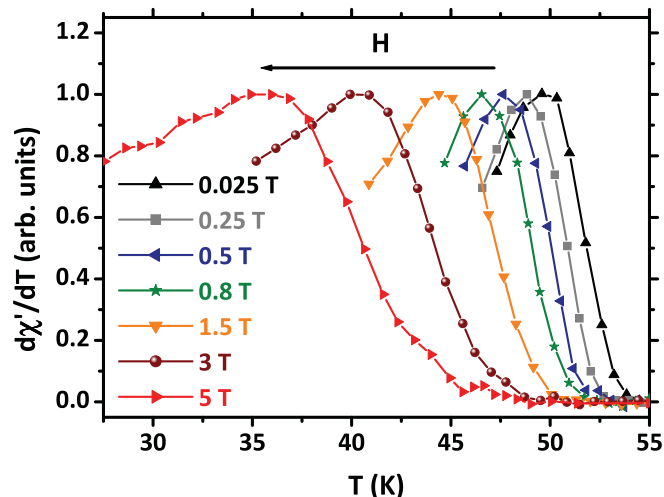


FIG. 3. (Color online) Temperature dependence of the first derivative of the real component of ac susceptibility χ' ($H_{ac} = 1.5 \times 10^{-4}$ T, $\nu_m = 37$ Hz) with respect to temperature at different applied magnetic fields. All the single curves were independently normalized to the corresponding maximum derivative value.

will be focusing on only the intragrain intrinsic dynamical properties. The stronger signal amplitude, moreover, made it reasonable to investigate the peak in the χ' derivative instead of the maximum in χ'' .

Figure 3 shows the temperature evolution of the normalized first derivative of the real component χ' of the ac susceptibility on the application of different values of static magnetic field H . In these measurements, both the alternating field and the working frequency were kept fixed at $H_{ac} = 1.5 \times 10^{-4}$ T and $\nu_m = 37$ Hz, respectively. The effect of increasing H is a clear shift of T_p toward lower values. At each applied H a clear dependence of T_p on ν_m was evidenced, as discussed later on. Some scans with H_{ac} values in the range $(0.0675\text{--}1.5) \times 10^{-4}$ T were also performed at the representative values $H = 0.025, 0.25$ and 5 T (data not shown). Within the experimental error, no dependence of T_p on H_{ac} was evidenced.

III. ANALYSIS AND DISCUSSION

The raw M_{dc} vs. T data reported in Fig. 1 were fitted by the function (see dashed curves in Fig. 1)

$$M_{dc}(T, H) = M_{sc} \left[1 - \left(\frac{T}{T_c} \right)^\alpha \right]^\beta + C_{cw} \frac{H}{T - T_N} + M_0(H) \quad (2)$$

where the first term is the diamagnetic Meissner response (empirically represented by a two-exponent mean-field function) and the second one is the Curie–Weiss paramagnetic contribution. The last term accounts for all the sources of T -independent magnetism, ranging from Pauli- and Van Vleck-like paramagnetism to a small contribution of magnetic impurities (e.g., Fe_2As).³⁹ A detailed analysis of the results of the fitting procedure according to Eq. (2) will be presented in another work.⁴⁰

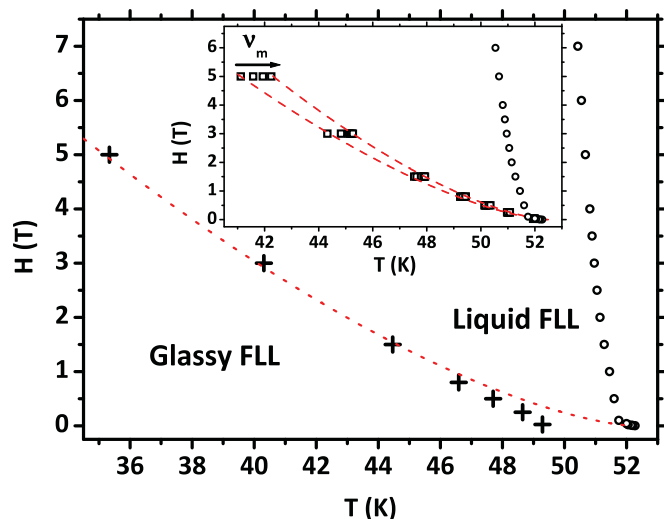


FIG. 4. (Color online) Phase diagram associated with the FLs. A glassy phase of FLs is separated from a liquid phase by the irreversibility line obtained from the field dependence of the maximum slope of χ' [plus signs (+), relative to $H_{ac} = 1.5 \times 10^{-4}$ T, $\nu_m = 37$ Hz]. The red dotted line is a best fit according to Eq. (4). Circles (o) track the behavior of H_{c2} as measured from dc magnetization data. Inset: comparison of the diamagnetic onset measured from dc magnetization (o) and ac susceptibility (\square) with $H_{ac} = 1.5 \times 10^{-4}$ T and $\nu_m = 37\text{--}1488$ Hz. The red dashed lines are best fits of data at $\nu_m = 37$ Hz and $\nu_m = 1488$ Hz according to Eq. (4).

Results from both SQUID magnetometry and ac susceptibility are summarized in the phase diagram shown in Fig. 4.

From the $T_c(H)$ data obtained from M_{dc} vs. T curves (see Fig. 1) it was possible to derive the temperature dependence of the upper critical field H_{c2} (see open circles in Fig. 4). A linear fit of the H_{c2} vs. T data deduced from magnetization data gives a slope $dH_{c2}/dT = 7.47 \pm 0.15$ T/K, in agreement with what was found in compounds of the same family from magnetoresistivity data,^{21,41} even if much lower slope values were reported from calorimetric measurements on single crystals of Nd-based 1111 superconductors.⁴² Then, in the simplified assumption of single-band superconductivity, through the Werthamer, Helfand and Hohenberg relation⁴³

$$H_{c2}(T = 0\text{K}) \simeq 0.693 \times T_c \left. \frac{dH_{c2}}{dT} \right|_{T \simeq T_c}, \quad (3)$$

it is possible to estimate $H_{c2} \simeq 270$ T in the limit of vanishing T .

A comparison between the diamagnetic onset temperature as obtained from ac susceptibility at different frequencies (see exemplifying raw data in Fig. 2) and the one obtained from static magnetization is plotted in the inset of Fig. 4. The onset in ac data was systematically found at lower temperatures than the corresponding dc diamagnetic onset. Dashed lines represent the empirical power-law fitting function

$$H \propto (1 - T/T_c)^\beta, \quad \beta = 3/2, \quad (4)$$

well describing experimental data at each value of the ac field frequency ν_m . Such a functional form characterized by

$\beta = \frac{4}{3} - \frac{3}{2}$ is known to describe the irreversibility line in the $H - T$ phase diagram of cuprates.⁴⁴

Plus signs in the phase diagram in Fig. 4 refer to the points $T = T_p$ of maximum slope of χ' vs. T curves ($H_{ac} = 1.5 \times 10^{-4}$ T and $\nu_m = 37$ Hz; see Fig. 3) corresponding, as already explained in Sec. II, to the maximum of χ'' vs. T associated with intrinsic intragrain losses. These data divide the phase diagram into two main regions, following the interpretation of the χ'' peak in term of resonant absorption of energy in a thermally activated flux-creep model.³⁰ In the high- T and high- H regions the FLs are in a reversible state, that is, they are responding to the external ac perturbation (liquid FLs). On the other hand, in the low- T and low- H region vortices are arranged in a glassy-like frozen state that gives rise to a non-reversible response and to dissipation, linked to the nonzero values assumed by χ'' . T_p vs. H points associated with the lowest accessible frequency ν_m are thus expected to belong to the irreversibility line (or de Almeida – Thouless line) of the FL phase diagram. As in the case of the diamagnetic onset in χ' (see Fig. 4, inset), Eq. (4) nicely fits the field dependence of T_p in the $H > 0.8$ T limit (see the dotted line in Fig. 4).

A logarithmic dependence of $1/T_p$ vs. ν_m at every fixed H is evidenced over the explored frequency range (see, for example, $H = 1.5$ T data in the inset of Fig. 5). Data can then be fitted within a thermally activated framework by the formula (red dashed line in the inset of Fig. 5)

$$\frac{\nu_m}{\nu_0} = \exp\left(-\frac{U_0(H)}{k_B T_p|_{\nu=\nu_m}}\right), \quad (5)$$

from which it can be observed that the logarithmic behavior of $1/T_p$ is mainly controlled by the parameter U_0 , playing the role of an effective depinning energy barrier in a thermally activated flux creep model. The parameter ν_0 takes the meaning of a intravalley characteristic frequency associated with the motion of the vortices around their equilibrium position in the pinning centers.

The advantage of extracting the value of U_0 from ac susceptibility data, if compared for instance with magnetoresistance data, is that the former is an almost isothermal estimate. Temperature, in fact, varies at most by 1 K as a function of ν_m at the highest applied H (see Fig. 5, inset) so that it is possible to determine U_0 at a temperature $T^*(H)$ with a maximum uncertainty of 0.5 K. This fact will be of interest when deriving the critical current density value, as it will be shown later on.

Data at different static magnetic fields can be fitted according to this model, giving the results reported in Fig. 5, where the H dependence of the effective depinning energy barrier U_0 is shown. Beyond an overall sizable reduction of U_0 with increasing H , a crossover between two different regimes can be clearly observed at $H \gtrsim 0.5$ T. At high fields the data are well described by a $1/H$ dependence, a well-known result in high- T_c cuprate superconductors, observed by means of several techniques, ranging from NMR⁴⁵ to ac magnetometry⁴⁶ and magnetoresistivity.³⁰ A naive explanation of this behavior can be obtained in terms of the balance between the Gibbs free energy of the system and the energy required for the motion of a FLs bundle.⁴⁷ In this framework, the crossover between the two different trends of U_0 vs. H shown in

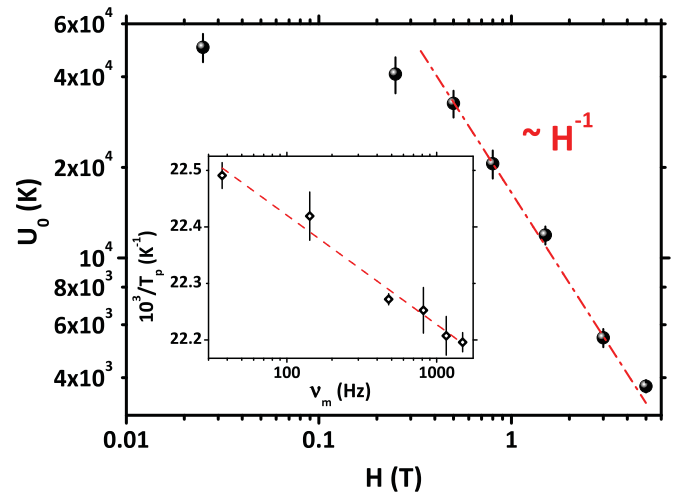


FIG. 5. (Color online) Magnetic field dependence of the effective depinning energy barrier. The red dashed-dotted line is a best fit of data according to a $1/H$ dependence for $H \gtrsim 0.5$ T. Inset: frequency dependence of $1/T_p$. Data refer to $H = 1.5$ T with the alternating field amplitude fixed to $H_{ac} = 1.5 \times 10^{-4}$ T. The red dashed line is a best fit of the experimental data according to Eq. (5).

Fig. 5 can be interpreted as the transition from a basically single-flux line response at low H values to a collective response of vortices for $H > 0.5$ T. A similar phenomenology was recently reported from magnetoresistivity data on a single crystal of O-deficient $\text{SmFeAsO}_{0.85}$ and on powder samples of La-based and Ce-based 1111 superconductors.^{13,14} The crossover between different regimes was observed at $H \simeq 1$ T in La-based samples and at much higher magnetic fields in Ce-based samples and in $\text{SmFeAsO}_{0.85}$ ($H \simeq 3$ T). However, U_0 values are typically 1 order of magnitude lower in La- and Ce-based superconductors. Comparing the sets of data for U_0 derived from magnetoresistivity and here from ac

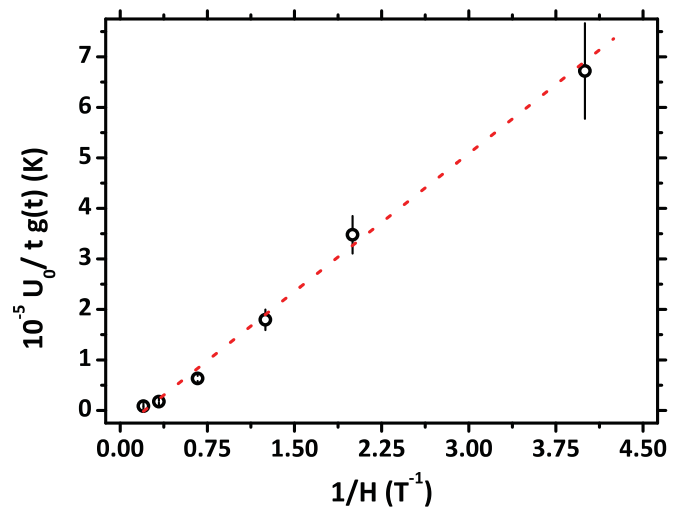


FIG. 6. (Color online) Plot of the effective energy barrier normalized with respect to the reduced temperature function $tg(t)$ (see text) as a function of the inverse applied static field. The slope of the linear fit (see red dotted curve) is directly proportional to the critical current density extrapolated at $T = 0$ K and $H = 0$ T.

susceptibility in Sm-based samples, the numerical agreement is very good for $H \gtrsim 1$ T.

In the $1/H$ regime, Tinkham⁴⁷ extended previous works by Yeshurun and Malozemoff^{44,48} showing that the relation for the normalized effective depinning energy barrier

$$\frac{U_0(t, H)}{t} \simeq \frac{K J_{c0}(0)}{H} g(t) \quad (6)$$

holds also for granular samples. Here U_0 is expressed in K, t is the reduced temperature $t \equiv T/T_c$, $g(t) \equiv 4(1-t)^{3/2}$, $J_{c0}(t)$ quantifies the critical current density at $H=0$ and $T=tT_c$, and the constant K is defined as $K \equiv 3\sqrt{3}\Phi_0^2\beta/2c$, Φ_0 being the flux quantum, c the speed of light, and β a numerical constant close to unit value. Equation (6) is derived in the simplified assumption of a two-fluid model.⁴⁷ By assuming that this empirical scenario can describe also the system under current investigation, from ac susceptibility it is possible to directly extrapolate the value of $J_{c0}(0)$. $U_0(H)$, as already noticed above, is almost isothermally estimated and can then be expressed as $U_0(t^*, H)$. By now plotting $U_0/t^*g(t^*)$ as a function of $1/H$ (see Fig. 6), from a linear fit of data it is possible to extract from Eq. (6) the value $J_{c0}(0) = (2.25 \pm 0.05) \times 10^7$ A/cm², having assumed $\beta = 1$. This rather high value is in agreement with estimates of the critical current density J_c evaluated by inductive measurements in similar Sm-based samples³⁸ and also with

the direct measurement of this quantity in Sm-based 1111 single crystals in the $T \rightarrow 0$ K and $H \rightarrow 0$ T limit.¹²

IV. CONCLUSIONS

The $H - T$ phase diagram of the flux lines in a powder sample of optimally doped SmFeAsO_{0.8}F_{0.2} was investigated by means of both ac and dc susceptibility measurements. The irreversibility line separating a liquid from a glassy phase was deduced and the activation depinning energy U_0 as a function of the external magnetic field derived in the framework of a thermally activated flux-creep theory. A $1/H$ dependence of U_0 for $H \gtrsim 0.5$ T, typical of collective motion of flux lines, has been evidenced. From the U_0 vs. H behavior a value of $J_{c0}(0) \sim 2 \times 10^7$ A/cm² has been extrapolated for the critical depinning current at both zero field and zero temperature. From this result we confirm that high intrinsic critical depinning current density values seem to be a peculiar feature of these systems, possibly making them good candidates for technological applications.

ACKNOWLEDGMENTS

M. J. Graf, A. Rigamonti, and L. Romanò are gratefully acknowledged for stimulating discussions. We thank C. Pernechele and D. Zola for useful help and suggestions about ac susceptibility measurements.

¹Y. Kamihara, H. Hiramatsu, M. Hirano, R. Kawamura, H. Yanagi, T. Kamiya, and H. Hosono, *J. Am. Chem. Soc.* **128**, 10012 (2006).

²Y. Kamihara, T. Watanabe, M. Hirano, and H. Hosono, *J. Am. Chem. Soc.* **130**, 3296 (2008).

³H. D. Lumsden and A. D. Christianson, *J. Phys. Cond. Matter* **22**, 203203 (2010).

⁴D. C. Johnston, *Adv. Phys.* **59**, 803 (2010).

⁵H. Luetkens, H.-H. Klauss, M. Kraken, F. J. Litterst, T. Dellmann, R. Klingeler, C. Hess, R. Khasanov, A. Amato, C. Baines, M. Kosmala, O. J. Schumann, M. Braden, J. Hamann-Borrero, N. Leps, A. Kondrat, G. Behr, J. Werner, and B. Büchner, *Nature Mat.* **8**, 305 (2009).

⁶S. Sanna, R. De Renzi, G. Lamura, C. Ferdeghini, A. Palenzona, M. Putti, M. Tropeano, and T. Shiroka, *Phys. Rev. B* **80**, 052503 (2009).

⁷S. Sanna, R. De Renzi, T. Shiroka, G. Lamura, G. Prando, P. Carretta, M. Putti, A. Martinelli, M. R. Cimberle, M. Tropeano, and A. Palenzona, *Phys. Rev. B* **82**, 060508(R) (2010).

⁸G. Prando, P. Carretta, A. Rigamonti, S. Sanna, A. Palenzona, M. Putti, and M. Tropeano, *Phys. Rev. B* **81**, 100508(R) (2010).

⁹L. Pourovskii, V. Vildosola, S. Biermann, and A. Georges, *Europhys. Lett.* **84**, 37006 (2008).

¹⁰L. Sun, X. Dai, C. Zhang, W. Yi, G. Chen, N. Wang, L. Zheng, Z. Jiang, X. Wei, Y. Huang, J. Yang, Z. Ren, W. Lu, X. Dong, G. Che, Q. Wu, H. Ding, J. Liu, T. Hu, and Z. Zhao, *Europhys. Lett.* **91**, 57008 (2010).

¹¹G. Blatter, M. V. Feigel'man, V. B. Geshkenbein, A. I. Larkin, and V. M. Vinokur, *Rev. Mod. Phys.* **66**, 1125 (1994).

¹²P. J. W. Moll, R. Puzniak, F. Balakirev, K. Rogacki, J. Karpinski, N. D. Zhigadlo, and B. Batlogg, *Nature Mat.* **9**, 628 (2010).

¹³H.-S. Lee, M. Bartkowiak, J. S. Kim, and H.-J. Lee, *Phys. Rev. B* **82**, 104523 (2010).

¹⁴M. Shahbazi, X. L. Wang, C. Shekhar, O. N. Srivastava, and S. X. Dou, *Supercond. Sci. Technol.* **23**, 105008 (2010).

¹⁵N. Y. Panarina, Y. I. Talanov, T. S. Shaposhnikova, N. R. Beysengulov, E. Vavilova, G. Behr, A. Kondrat, C. Hess, N. Leps, S. Wurmehl, R. Klingeler, V. Kataev, and B. Buchner, *Phys. Rev. B* **81**, 224509 (2010).

¹⁶Y. J. Jo, J. Jaroszynski, A. Yamamoto, A. Gurevich, S. C. Riggs, G. S. Boebinger, D. Larbalestier, H. H. Wen, N. D. Zhigadlo, S. Katrych, Z. Bukowski, J. Karpinski, R. H. Liu, H. Chen, X. H. Chen, and L. Balicas, *Phys. C* **469**, 566 (2009).

¹⁷C. J. van der Beek, G. Rizza, M. Konczykowski, P. Fertey, I. Monnet, T. Klein, R. Okazaki, M. Ishikado, H. Kito, A. Iyo, H. Eisaki, S. Shamoto, M. E. Tillman, S. L. Bud'ko, P. C. Canfield, T. Shibauchi, and Y. Matsuda, *Phys. Rev. B* **81**, 174517 (2010).

¹⁸A. Yamamoto, A. A. Polyanskii, J. Jiang, F. Kametani, C. Tarantini, F. Hunte, J. Jaroszynski, E. E. Hellstrom, P. J. Lee, A. Gurevich, D. C. Larbalestier, Z. A. Ren, J. Yang, X. L. Dong, W. Lu, and Z. X. Zhao, *Supercond. Sci. Technol.* **21**, 095008 (2008).

¹⁹D. Ahmad, I. Park, G. C. Kim, J. H. Lee, Z.-A. Ren, and Y. C. Kim, *Phys. C* **469**, 1052 (2009).

²⁰D. H. Ryan, J. M. Cadogan, C. Ritter, F. Canepa, A. Palenzona, and M. Putti, *Phys. Rev. B* **80**, 220503(R) (2009).

²¹I. Pallecchi, C. Fanciulli, M. Tropeano, A. Palenzona, M. Ferretti, A. Malagoli, A. Martinelli, I. Sheikin, M. Putti, and C. Ferdeghini, *Phys. Rev. B* **79**, 104515 (2009).

- ²²P. H. Kes, J. Aarts, J. van der Beek, and J. A. Mydosh, *Supercond. Sci. Technol.* **1**, 242 (1989).
- ²³C. P. Bean, *Phys. Rev. Lett.* **8**, 250 (1962).
- ²⁴C. P. Bean, *Rev. Mod. Phys.* **36**, 31 (1964).
- ²⁵M. C. Frischherz, F. M. Sauerzopf, H. W. Weber, M. Murakami, and G. A. Emel'chenko, *Supercond. Sci. Technol.* **8**, 485 (1997).
- ²⁶J. R. Clem, in *Magnetic Susceptibility of Superconductors and Other Spin Systems*, edited by R. A. Hein, T. L. Francavilla, and D. H. Liebenberg (Plenum, New York, 1991), p. 177
- ²⁷V. B. Geshkenbein, V. M. Vinokur, and R. Fehrenbacher, *Phys. Rev. B* **43**, 3748(R) (1991).
- ²⁸E. H. Brandt, in *The Vortex State*, edited by N. Bontemps, Y. Bruynseraede, G. Deutscher, and A. Kapitulnik (Kluwer Academic, Amsterdam, 1994), p. 125.
- ²⁹F. Gmöröy, *Supercond. Sci. Technol.* **10**, 523 (1997).
- ³⁰T. T. M. Palstra, B. Batlogg, R. B. van Dover, L. F. Schneemeyer, and J. V. Waszczak, *Phys. Rev. B* **41**, 6621 (1990).
- ³¹M. Tinkham, *Phys. B* **169**, 66 (1991).
- ³²P. W. Anderson, and Y. B. Kim, *Rev. Mod. Phys.* **36**, 39 (1964).
- ³³M. Tinkham, *Introduction to Superconductivity* (McGraw-Hill, New York, (1996).
- ³⁴M. Nikolo, R. B. Goldfarb, *Phys. Rev. B* **39**, 6615 (1989).
- ³⁵M. Nikolo, *Am. J. Phys.* **63**, 57 (1995).
- ³⁶B. V. Kumaraswamy, R. Lal, and A. V. Narlikar, *Phys. Rev. B* **52**, 1320 (1995).
- ³⁷K.-H. Müller, *Phys. B* **168**, 585 (1990).
- ³⁸A. Yamamoto, J. Jiang, F. Kametani, A. Polyanskii, E. Hellstrom, D. Larbalestier, A. Martinelli, A. Palenzona, M. Tropeano, and M. Putti, *Supercond. Sci. Technol.* **24**, 045010 (2011).
- ³⁹M. R. Cimperle, F. Canepa, M. Ferretti, A. Martinelli, A. Palenzona, A. S. Siri, C. Tarantini, M. Tropeano, and C. Ferdeghini, *Magn. Mat.* **321**, 3024 (2009).
- ⁴⁰G. Prando, P. Carretta, A. Lascialfari, A. Rigamonti, S. Sanna, A. Palenzona, M. Putti, and M. Tropeano, to be published.
- ⁴¹J. Jaroszynski, S. C. Riggs, F. Hunte, A. Gurevich, D. C. Larbalestier, G. S. Boebinger, F. F. Balakirev, A. Migliori, Z. A. Ren, W. Lu, J. Yang, X. L. Shen, X. L. Dong, Z. X. Zhao, R. Jin, A. S. Sefat, M. A. McGuire, B. C. Sales, D. K. Christen, and D. Mandrus, *Phys. Rev. B* **78**, 064511 (2008).
- ⁴²U. Welp, R. Xie, A. E. Koshelev, W. K. Kwok, P. Cheng, L. Fang, and H.-H. Wen, *Phys. Rev. B* **78**, 140510(R) (2008).
- ⁴³N. R. Werthamer, E. Helfand, and P. C. Hohenberg, *Phys. Rev.* **147**, 295 (1966).
- ⁴⁴A. P. Malozemoff, T. K. Worthington, Y. Yeshurun, F. Holtzberg, and P. H. Kes, *Phys. Rev. B* **38**, 7203(R) (1988).
- ⁴⁵A. Rigamonti, F. Borsa, and P. Carretta, *Rep. Prog. Phys.* **61**, 1367 (1998).
- ⁴⁶J. H. P. M. Emmen, V. A. M. Brabers, and W. J. M. de Jonge, *Phys. C* **176**, 137 (1991).
- ⁴⁷M. Tinkham, *Phys. Rev. Lett.* **61**, 1658 (1988).
- ⁴⁸Y. Yeshurun and A. P. Malozemoff, *Phys. Rev. Lett.* **60**, 2202 (1988).